ELSEVIER

Journal of Alloys and Compounds 408–412 (2006) 1205–1209

Journal of ALLOYS AND COMPOUNDS

www.elsevier.com/locate/jallcom

Structure and magnetic properties of $Ca_xLa_{2-x}MnIrO_6$ solid solution

Md. Tahidul Haque, Hirohisa Satoh, Naoki Kamegashira *

Department of Materials Science, Toyohashi University of Technology, Tempaku-cho, Toyohashi 441-8580, Japan

Received 30 July 2004; received in revised form 24 November 2004; accepted 15 December 2004
Available online 13 June 2005

Abstract

Synthesis of $Ca_xLa_{2-x}MnIrO_6$ ($1.5 \leq x \leq 1.9$) solid solution was tried in varying atmospheric conditions. The solid solution has the perovskite-type structure characterized by Rietveld refinement of powder X-ray diffraction data. An orthorhombic space group *Pnma* (no. 62) with cation-disordered distribution over A- and B-sites was determined for all the compositions of the solid solution. Some magnetic ordering for the solid solution was observed at low temperature by the magnetic susceptibility measurement and the existence of hysteresis loops ascertains that the ordering observed in the temperature dependence of susceptibility is ferromagnetic. The effective magnetic moment (μ_{eff}) decreases sharply with the increase of Ca^{2+} ion indicating the formation of non-magnetic Ir^{5+} ion produced due to cationic charge deficiency.

Keywords: Crystal structure and symmetry; X-ray diffraction; Magnetic measurements

1. Introduction

Perovskite-type oxides containing rare earth element and manganese have been noted from various interests of physical and chemical properties such as colossal magnetoresistance (CMR) effect [1,2] and potential application to electrode materials for solid oxide fuel cell (SOFC) [3,4]. Perovskite compounds having double cations in B-site have also been the subject of many investigations. Compounds of type $A_2B'B''O_6$ tend to adopt a perovskite-type structure when A is a large cation capable of 12-fold coordination with oxygen, while B′ and B″ are smaller cations suitable for octahedral coordination [5]. Among these perovskites, the complex oxides La_2(Mn, Rh)O_6 in various combination of 3d transition metal manganese with 4d transition metal rhodium in B-site of the perovskite structure [6,7] have been studied. The consequences for the materials of perovskite structure in combination of 5d transition metal manganese with 3d transition metal iridium in B-site has in the past been the subject of few publications. The valence state of iridium in solid compounds has primarily +4 oxidation state, although Ir^{5+} has been identified in $KIrO_3$ [8] and $Ba_{0.5}IrO_3$ [9], and $La_3Ir_3O_{11}$ [10] is a mixed valence compound. The properties of IrO_2 as an anode material include high electrocatalytic activity, high electron conductivity and high stability at various environments. The oxides of Ir^{4+} are often metallic, for example IrO_2, but a more localized electron behavior is observed when this cation is located in a more complex structure as in mixed oxides of perovskite [11] or pyrochlore type [12]. Therefore, the study of the structure and properties of mixed oxides containing manganese and iridium is of interest.

It has been reported [13] that the formation of perovskite structure containing Mn and Ir in B-sites in normal atmospheric condition is very difficult. Demazeau [14] reported $LaMnIrO_6$ to be synthesized from the stoichiometric mixture of La_2O_3, IrO_2 and MnO in a high-pressure–high-temperature route [15]. In this study, we adopted all possible conditions in an ambient pressure process to synthesize La_2MnIrO_6 but no condition led to one single phase. In this situation, substitution of some divalent alkaline earth metals for La^{3+} could lead to one single phase as Blasse [16] reported the existence of $SrLaMnIrO_6$, $SrLaMnTiO_6$ and $SrLaFeIrO_6$ phases. Fractional substitution of Ca^{2+} for La^{3+} to synthe-

* Corresponding author. Tel.: +81 532 44 6797; fax: +81 532 48 5833.
E-mail address: nkarnegas@tutms.tut.ac.jp (N. Kamegashira).

0925-8388/$ – see front matter © 2005 Elsevier B.V. All rights reserved.
doi:10.1016/j.jallcom.2004.12.131

size the expected compounds was tried in various preparation conditions and it is found that single phases are possible only for Ca-rich region ($1.5 \leq x \leq 1.9$) in $Ca_xLa_{2-x}MnIrO_6$ and the structure analysis and magnetic properties of this solid solution have been the focus of this study.

2. Experimental

Polycrystalline samples of $Ca_xLa_{2-x}MnIrO_6$ solid solution were synthesized by the solid-state reaction method from stoichiometric mixtures of $CaCO_3$ (99.99%, Rare Metallic Co. Ltd.), La_2O_3 (99.99%, Rare Metallic Co. Ltd.), Mn_2O_3 (99.99%, Koujundo Chemical Laboratory Co. Ltd.) and IrO_2 (more than 99%, Tanaka Precious Metal Industry). The starting materials were pretreated to adjust stoichiometry by the following method: $CaCO_3$ was heated at 673 K in CO_2 flow for 24 h, La_2O_3 was heated at 1273 K in Ar flow for 24 h, Mn_2O_3 was heated at 1073 K in air for 72 h and quenched to room temperature [17] and IrO_2 was heated at 1273 K in air for 48 h. A mixture of an appropriate molar ratio of these starting materials was pressed into pellet and was heated in air at various temperatures, until equilibrium conditions were obtained. The grinding and heating processes were repeated to get a homogeneous specimen.

Single phase of the products was identified by X-ray powder diffraction method. The powder X-ray diffraction data were collected with Cu Kα radiation using MAC MXP^{18} powder X-ray diffractometer equipped with a single crystal graphite monochrometer. The conditions for data collection were as follows: 2θ range, $10^\circ \leq 2\theta \leq 120^\circ$; step width ($2\theta$), 0.04°; sampling time, 2 s. The powder X-ray diffraction patterns obtained were analyzed by Rietveld method using the program RIETAN [18,19].

Magnetic measurements were carried out on a Quantum Design MPMS-7 SQUID magnetometer. DC susceptibility measurements were made under both ZFC (zero-field-cooled) and FC (field-cooled) conditions from liquid helium temperature to room temperature at 1000 G. FC curves were collected by cooling the samples under the field of 1000 G. Magnetization was measured at 4 K with changing field between ±30,000 G.

3. Results and discussion

3.1. Synthesis of phases

All possible conditions to synthesize the compositions of $Ca_xLa_{2-x}MnIrO_6$ ($0 \leq x \leq 2.0$) solid solution were tried. Firstly, a trial to synthesize La_2MnIrO_6 at various atmospheres was unsuccessful since IrO_2 decomposes into metallic Ir easily under low oxygen partial pressure at high temperature. Over much investigation air pressure compatible to suppress the decomposition of IrO_2 was selected. But any conditions to synthesize La_2MnIrO_6 in air at various temperatures led to multiphase. In all cases impurity peaks of La_2MnO_4 along with some unreacted La_2O_3 and IrO_2 are seen in the X-ray diffraction patterns. Adoption of stoichiometric MnO instead of Mn_2O_3 as one of the starting materials led the same impurities to appear. Flowing of oxygen gas instead of air did not reduce the impurities anymore. Iridium being tetravalent, a step to synthesize Mn-rich compounds of $La_2(Mn, Ir)O_6$ solid solution was taken but to no avail. Partial substitution of Ca^{2+} for La^{3+} induced whole La_2O_3 and IrO_2 to get reacted but led to grow new impurities as $La_2MnO_{4.15}$ and $CaIrO_3$ in the range $0 < x \leq 1.3$ for $Ca_xLa_{2-x}MnIrO_6$ solid solution. Synthesis of single phases of $Ca_xLa_{2-x}MnIrO_6$ ($1.5 \leq x \leq 1.9$) was successful and heating the palletized sample at 1273 K in air for 48 h was found to be the ideal condition to form single phase for $Ca_{1.5}La_{0.5}MnIrO_6$. Calcinations at temperature lower than 1273 K left some IrO_2 unreacted. But with the increase of the fractional content of Ca^{2+}, a little higher temperature was needed for the reactions to form single phases. Consequently, $Ca_{1.7}La_{0.3}MnIrO_6$ and $Ca_{1.9}La_{0.1}MnIrO_6$ were synthesized at 1323 K and 1373 K in air. Attempts to prepare pure Ca_2MnIrO_6 in the same way gave rise to some unknown impurities.

3.2. Structure analysis

For the single phases of $Ca_xLa_{2-x}MnIrO_6$ ($1.5 \leq x \leq 1.9$) solid solution, the most probable space group estimated by the CELL program [20,21] belongs to orthorhombic symmetry with the space group *Pnma* (no. 62). When Rietveld analysis using the program RIETAN was carried out using this space group, the calculated diffraction patterns showed better agreements with the observed patterns resulting in reasonable *R* (Reliable factor) values than in other space groups. Refinement of the structure in *Pnma* led to good fit for atomic coordination. In the model of the structure for Rietveld refinement with *Pnma,* the assigned occupation sites were 4c for Ca/La, 4b for Mn/Ir, 4c for O1, 8d for O2 and a random distribution of Ca^{2+} and La^{3+} ions over A-sites and Mn^{3+} and Ir^{4+} ions over B-sites were assumed. The overall isotropic thermal parameter was used throughout this calculation. Cation ordering over B-sites plays an important role for its magnetic and electrical properties. The space group *Pnma* does not allow cation ordering over B-sites. Cation ordering in B-site is known for several $AA'BB'O_6$ mixed oxides [22–24], and leads to monoclinic space group $P2_1/n$ with a monoclinic angle β very close to 90°. Taking this into account, Rietveld refinement with the space group $P2_1/n$ (no. 14) assuming ordered model of Mn^{3+} and Ir^{4+} ions over B-sites was conducted. The Ca^{2+} and La^{3+} cations were assumed to be randomly distributed over the A-sites. The refinement with $P2_1/n$ led to serious misfit for the peaks and the system of equations became numerically unstable with higher *R*-values. Thus an orthorhombic space group *Pnma* with cation-disordered distribution over A- and B-sites was finally determined for $Ca_xLa_{2-x}MnIrO_6$ ($1.5 \leq x \leq 1.9$) solid

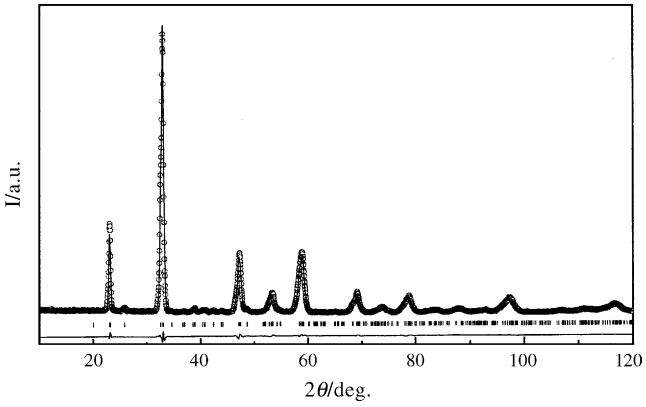

Fig. 1. Observed X-ray diffraction intensity (circle) and calculated curve (line) of $Ca_{1.5}La_{0.5}MnIrO_6$ for the space group *Pnma*. The bottom curve is the difference of patterns, $y_{obs} - y_{cal}$, and the small bars indicate the angular positions of the allowed Bragg reflections.

solution. The observed and calculated profiles by Rietveld refinement with *Pnma* for $Ca_{1.5}La_{0.5}MnIrO_6$ are shown in Fig. 1.

The variation of the lattice parameters and volume of the solid solution as a function of Ca content is shown in Fig. 2. The lattice constants decrease continously with the increase of Ca content that results in decreasing the unit cell volume. The ionic radii of La^{3+} and Ca^{2+} in 12 coordination are 1.36 Å and 1.34 Å, respectively, as reported by Shannon [25]. Although the ionic radius of Ca^{2+} is little smaller than that of La^{3+}, the lattice constants as well as the unit cell volume decrease quite sharply with the increase of Ca content as is seen in Fig. 2. This simply indicates the creation of Mn^{4+} or Ir^{5+} (possessing smaller ionic radius than Mn^{3+} or Ir^{4+}, respectively) produced due to cationic charge deficiency resulting from the substitution of Ca^{2+} for La^{3+}.

Table 1 shows the crystallographic data and interatomic distances with bond angles of $Ca_xLa_{2-x}MnIrO_6$ ($1.5 \le x \le 1.9$) for the space group *Pnma*. The average Mn/Ir–O and La/Ca–O distances decrease continuously with the increase of Ca content, as is the case of lattice constants and unit cell volume. Fractional atomic coordinates of $Ca_xLa_{2-x}MnIrO_6$ ($1.5 \le x \le 1.9$) for the space group *Pnma* are given in Table 2. As is shown in this table, the atomic displacement of O1 from ideal cubic structure is considerably larger than that of O2 for La-rich compounds. Consequently the lattice distortion along Mn/Ir–O1 [0 1 0] for $Ca_{1.5}La_{0.5}MnIrO_6$ is the largest. The lattice distortion along this direction decreases with the increase of Ca content which resulted from the decrease of atomic displacement of O1 from ideal cubic structure. But the average tilting angle for the compounds of $Ca_xLa_{2-x}MnIrO_6$ ($1.5 \le x \le 1.9$) solid solution remains almost the same.

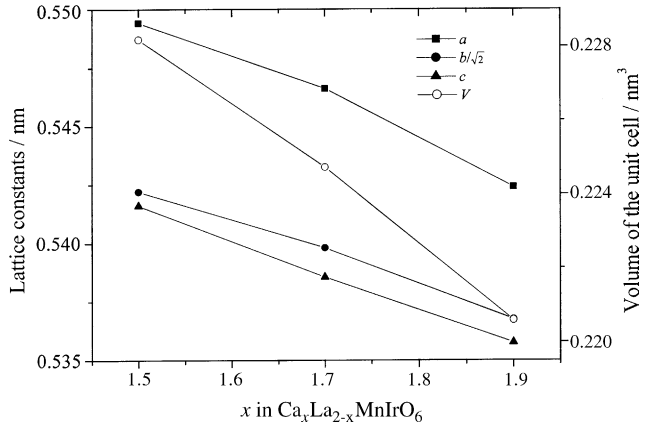

Fig. 2. Lattice constants and volume of the unit cell as a function of Ca content for $Ca_xLa_{2-x}MnIrO_6$ ($1.5 \le x \le 1.9$) solid solution.

Table 1
Crystallographic data and interatomic distances with bond angles of $Ca_xLa_{2-x}MnIrO_6$ ($1.5 \le x \le 1.9$) for the space group *Pnma*

	$Ca_{1.5}La_{0.5}MnIrO_6$	$Ca_{1.7}La_{0.3}MnIrO_6$	$Ca_{1.9}La_{0.1}MnIrO_6$
Lattice parameters			
a (nm)	0.54942(9)	0.54662(5)	0.54241(7)
b (nm)	0.7668(1)	0.76340(6)	0.75907(8)
c (nm)	0.54161(7)	0.53855(5)	0.53575(6)
V (nm^3)	0.228188	0.224731	0.220583
Reliability factors			
R_{WP} (%)	10.89	11.37	14.32
R_P (%)	8.56	8.52	10.96
R_E (%)	4.94	5.40	5.13
R_I (%)	4.18	3.88	4.64
R_F (%)	1.88	1.61	3.52
S ($=R_{WP}/R_E$)	2.20	2.11	2.79
Bond distances (nm)			
La/Ca–O1	0.328(6)	0.314(5)	0.303(8)
	0.313(5)	0.320(4)	0.301(7)
	0.217(6)	0.231(5)	0.235(8)
	0.256(5)	0.240(4)	0.251(7)
La/Ca–O2(l)	0.247(4) × 2	0.239(3) × 2	0.228(5) × 2
	0.255(5) × 2	0.271(4) × 2	0.260(6) × 2
La/Ca–O2(2)	0.322(4) × 2	0.328(3) × 2	0.334(5) × 2
	0.272(5) × 2	0.254(4) × 2	0.265(5) × 2
Mean (La/Ca–O) distance	0.2755	0.2741	0.2720
Mn/Ir–O1	0.203(2) × 2	0.199(l) × 2	0.195(2) × 2
Mn/Ir–O2(1)	0.192(6) × 2	0.191(4) × 2	0.196(5) × 2
Mn/Ir–O2(2)	0.200(6) × 2	0.201(4) × 2	0.199(6) × 2
Mean (Mn/Ir–O) distance	0.1983	0.1970	0.1967
Bond angles (°)			
Mn/Ir–O1–Mn/Ir	142(3)	148(3)	155(4)
Mn/Ir–O2(1)–Mn/Ir	159(2)	156(2)	151(2)
Mn/Ir–O2(2)–Mn/Ir	159(2)	156(2)	151(2)
Tilting angles (°)			
Along *b* [0 1 0]	19(2)	16(1)	13(2)
Along [1 0 $\bar{1}$]	11(1)	12(1)	15(1)
Along [1 0 1]	10(1)	12(1)	15(1)

The standard deviation of the last digit is given in parenthesis.

3.3. Magnetic properties

The magnetic susceptibility as a function of temperature for the end compounds of $Ca_xLa_{2-x}MnIrO_6$ ($1.5 \le x \le 1.9$)

Table 2
Fractional atomic coordinates of $Ca_xLa_{2-x}MnIrO_6$ ($1.5 \leq x \leq 1.9$) for the space group *Pnma*

Atom	Wychoff letter	*x/a*	*y/b*	*z/c*	B_{iso}, 10^{-2} nm^2 (overall)
For $Ca_{1.5}La_{0.5}MnIrO_6$					
Ca, La	4c	−0.040(1)	1/4	0.017(2)	0.15(8)
Mn, Ir	4b	0	0	1/2	
O1	4c	0.014(8)	1/4	0.62(1)	
O2	8d	0.203(8)	0.017(7)	0.211(9)	
For $Ca_{1.7}La_{0.3}MnIrO_6$					
Ca, La	4c	−0.042(1)	1/4	0.018(2)	0.20(7)
Mn, Ir	4b	0	0	1/2	
O1	4c	0.033(7)	1/4	0.596(9)	
O2	8d	0.222(7)	0.039(7)	0.208(7)	
For $Ca_{1.9}La_{0.1}MnIrO_6$					
Ca, La	4c	−0.041(2)	1/4	0.016(5)	0.3(1)
Mn, Ir	4b	0	0	1/2	
O1	4c	0.01(1)	1/4	0.57(1)	
O2	8d	0.199(9)	0.038(7)	0.19(1)	

The standard deviation of the last digit is given in parenthesis.

solid solution, measured at an applied magnetic field 1000 Oe, is shown in Fig. 3. The divergence of the ZFC and FC magnetic susceptibilities can be ascribed to the effect of magnetic field while cooling: on cooling in the absence of an applied field the magnetic moments orient randomly, whereas they tend to align themselves with the field resulting in an increased measured susceptibility when the cooling is repeated in the measuring field. The field dependence of susceptibility indicates the presence of ferromagnetic interactions at low temperature. Fig. 4 shows the magnetization as a function of magnetic field under ZFC condition for the compounds, measured at 4 K. Hysteresis loops are observed for both compounds and the existence of the loops ascertain that the orderings observed in the temperature dependence of susceptibility is ferromagnetic. Thus, the marked divergence of the ZFC and FC susceptibilities can be explained as the presence of weak ferromagnetism in an otherwise antiferromagnetic material. Since the absence of any long-range cationic order was confirmed by X-ray diffraction data it could be assumed that domains of short-range cationic order between Mn^{3+} and Ir^{4+} led to ferromagnetic properties with moderate intensity.

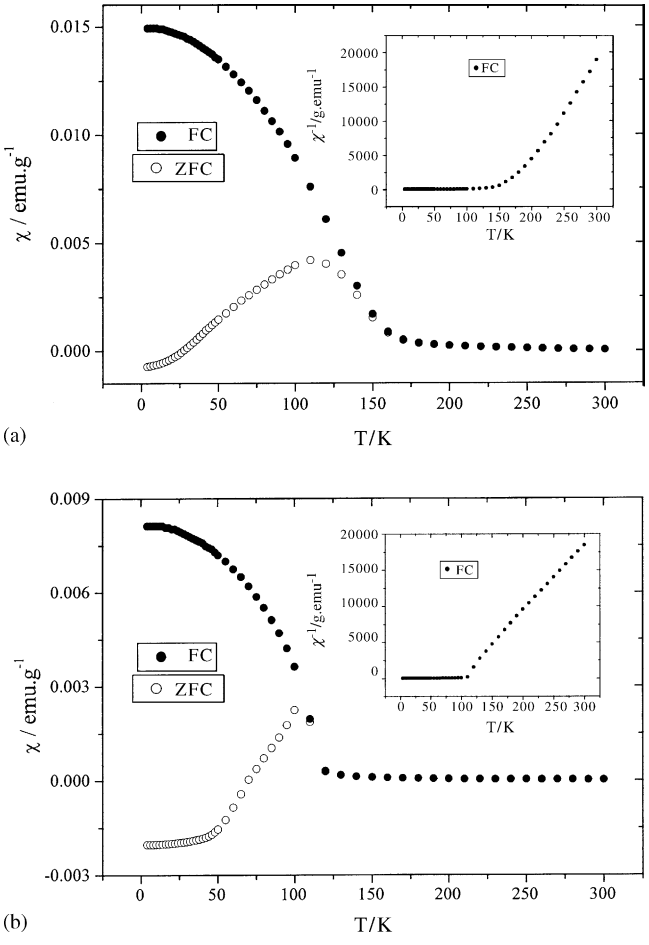

Fig. 3. Magnetic susceptibility as a function of temperature for (a) $Ca_{1.5}La_{0.5}MnIrO_6$ and (b) $Ca_{1.9}La_{0.1}MnIrO_6$. Inset: the inverse magnetic susceptibility as a function of temperature.

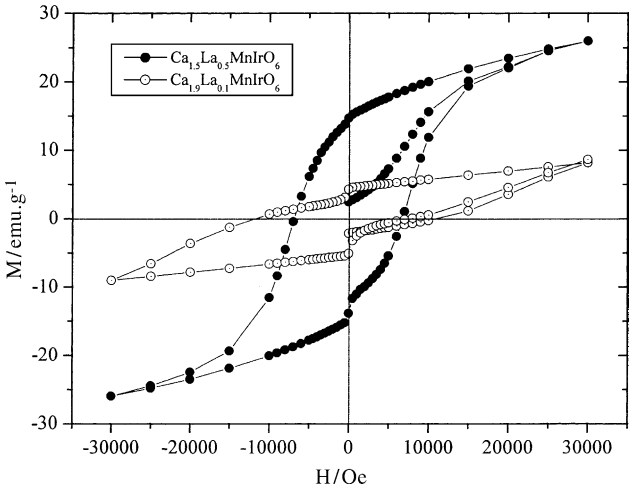

Fig. 4. Magnetization as a function of magnetic field measured at 4 K for both $Ca_{1.5}La_{0.5}MnIrO_6$ and $Ca_{1.9}La_{0.1}MnIrO_6$.

Curie temperatures (T_C) calculated from the susceptibility curves were about 140 K and 110 K for $Ca_{1.5}La_{0.5}MnIrO_6$ and $Ca_{1.9}La_{0.1}MnIrO_6$, respectively. T_C was determined by the numerical analysis of the point of inflection where the first derivative $\partial\chi/\partial T$ has a maximum T_C and the second derivative $\partial\chi^2/\partial T^2$ is zero [26]. Fitting of the reciprocal susceptibility in the paramagnetic region to a Curie–Weiss law leads to an effective magnetic moment of $\mu_{eff} = 3.60\,\mu_B$ per transition metal cation and Weiss constant of $\Theta = 172$ K for $Ca_{1.5}La_{0.5}MnIrO_6$ and $\mu_{eff} = 3.09\,\mu_B$ per cation and $\Theta = 95$ K for $Ca_{1.9}La_{0.1}MnIrO_6$. If both Mn^{3+} (high-spin) and Ir^{4+} (low-spin) obeyed the spin-only formula, the material would have an effective magnetic moment of $3.74\,\mu_B$ per cation. Therefore the observed effective magnetic moment for $Ca_{1.5}La_{0.5}MnIrO_6$ is reasonable for the localized $3d^4$ electron system in a high-spin configuration and $5d^5$ electron system in a low-spin configuration on an octahedral site and the positive Weiss constants are more consistent with the observation of low temperature ferromagnetism. But μ_{eff} as well as the intensity of ferromagnetism (Fig. 4) decreases sharply with the increase of Ca^{2+} ion indicating the formation of Ir^{5+} ion produced due to cationic charge deficiency. The Kotani theory [27,28] for a low-spin d^4 ion predicts that $\mu^2_{eff}[Ir(V)] = 72\,kT\,A^{-1}$ where A is the spin-orbit coupling constant for Ir(V). This leads to a non-magnetic ($j = 0$) ground state that results in decreasing the ferromagnetic interactions in $Ca_{1.9}La_{0.1}MnIrO_6$. Usually manganese ion is very notable for its change of valence state due to charge neutrality in compounds. So, it is probable that a part of Mn^{3+} was converted to Mn^{4+} due to cationic charge deficiency. But in such situation, the ferromagnetic intensity would have been enhanced because Mn^{3+}–O^{2-}–Mn^{4+} interaction is ferromagnetic.

Acknowledgements

This work was supported by the Grant-in-Aid for Scientific Research (B) (no. 13450 259) by Japan Society for the Promotion of Science. Thanks are due to the Research Center for Molecular Materials, the Institute for Molecular Science, Okazaki, for assistance in obtaining the magnetic properties at low temperature.

References

[1] S. Jin, T.H. Tiefel, M. McCormack, R.A. Fastnacht, R. Ramesh, L.H. Chen, Science 264 (1994) 413.
[2] R. von Helmolt, J. Wecker, B. Holzapfel, L. Schultz, K. Samwer, Phys. Rev. Lett. 67 (1993) 2331.
[3] N.M. Sammes, M.B. Phillips, O. Yamamoto, Proceedings of the Fourth International Symposium on Solid Oxide Fuel Cells (SOFC-IV), 1995, p. 472.
[4] A. Martinez-Juarez, L. Sanchez, E. Chinarro, P. Recio, C. Pascal, J.R. Jurado, Solid State Ionics 135 (2000) 525.
[5] F.K. Patterson, C.W. Moeller, R. Ward, Inorg. Chem. 2 (1963) 196.
[6] M.T. Haque, H. Satoh, N. Kamegashira, Mater. Lett. 58 (2004) 1571.
[7] M.T. Haque, H. Satoh, N. Kamegashira, Mater. Res. Bull. 39 (2004) 375.
[8] R. Hoppe, K. Glaes, J. Less-Common Met. 43 (1975) 129.
[9] A.W. Sleight, Mater. Res. Bull. 9 (1974) 1177.
[10] F. Abraham, J. Trehoux, D. Thomas, J. Less-Common Met. 63 (1979) 57.
[11] E.M. Ramos, I. Alvarez, M.L. Veiga, C. Pico, Mater. Res. Bull. 29 (1994) 881.
[12] A.W. Sleight, J.L. Gillson, Mater. Res. Bull. 6 (1971) 781.
[13] R.C. Currie, J.F. Vente, E. Frikkee, D.J.W. Ijdo, J. Solid State Chem. 116 (1995) 199.
[14] G. Demazeau, B. Siberchicot, S. Matar, C. Gayet, A. Largeteau, J. Appl. Phys. 75 (1994) 4617.
[15] G. Demazeau, Haute Pression et Biotechnologie, in: C. Balny, R. Hayashi, K. Heremans, P. Masson (Eds.), Coll. INSERM, vol. 224, John Libbey INSERM, Paris, 1992, p. 481.
[16] G. Blasse, J. Inorg. Chem. 27 (1965) 993.
[17] N. Kamegashira, Y. Miyazaki, H. Yamamoto, Mater. Chem. Phys. 11 (1984) 187.
[18] F. Izumi, J. Crystallogr. Jpn. 27 (1985) 23.
[19] F. Izumi, J. Minerallogr. Soc. Jpn. 17 (1985) 37.
[20] Y. Takaki, T. Taniguchi, K. Nakata, H. Yamaguchi, J. Ceram. Soc. Jpn. 97 (1989) 763.
[21] Y. Takaki, T. Taniguchi, K. Hori, J. Ceram. Soc. Jpn. 101 (1993) 373.
[22] S.H. Kim, P.D. Battle, J. Solid State Chem. 114 (1995) 174.
[23] T. Horikubi, H. Watanabe, N. Kamegashira, J. Alloys Compd. 274 (1998) 122.
[24] T. Horikubi, N. Kamegashira, J. Alloys Compd. 287 (1999) 62.
[25] R.D. Shannon, Acta Crystallogr. A32 (1976) 751.
[26] C. Schinzer, J. Phys. Chem. Solids 61 (2000) 1543.
[27] M. Kotani, J. Phys. Soc. Jpn. 4 (1949) 293.
[28] K. Hayashi, G. Demazeau, M. Pouchard, P. Hagenmuller, Mater. Res. Bull. 15 (1980) 461.